scientific reports

Check for updates

OPEN

Comprehensive multiomics profiling reveals the protective function of gypenosides against dextran sulfate sodium-induced colitis

Yuan Yang[1,3], Xinyuan Li[1,3], Fan Huang[1,3], Fuchao Cai[1], Xufeng Ning[1], Qilin Jiang[1], Lingshan Zhou[2], Bin Zeng[1]✉, Weiwei Zhou[1]✉ & Guangsheng Hu[1]✉

In this study, we determined whether gypenosides exert a therapeutic effect on colitis. We then explored the underlying mechanism of gypenosides in the treatment of ulcerative colitis (UC) via multiomics analyses. Dextran sulfate sodium (DSS) was used to establish a UC model in mice, and a subgroup of colitis model mice was subjected to gypenosides intervention. The inflammatory manifestations of the model and drug groups were determined via histological and molecular experiments. In addition, tissue and blood samples were collected for transcriptome and metabolomics analysis, respectively. Immunohistochemistry was used to detect the key proteins involved in UC pathogenesis and drug intervention. By combining transcriptomics and metabolomics assays, we explored one of the possible mechanisms by which gypenosides ameliorate UC in mice. Gypenosides treatment significantly alleviated clinical symptoms, prevented colon shortening, and decreased the disease activity index (DAI) in an 3% DSS-induced UC mouse model. Transcriptome sequencing revealed that the intestinal stem genes Ascl2 and Lgr5 ranked forefront in terms of differential expression before and after intervention with gypenosides. The metabolomics results suggest that the tricarboxylic acid cycle (TCA) and amino acid metabolism (AM) were the main metabolic pathways associated with UC and gypenosides treatment. Taken together, these results suggest that gypenosides may affect the biological activity of stem cells by regulating the tricarboxylic acid cycle and glutamine metabolism, promoting the repair of the damaged mucosa. In this study, we demonstrated that gypenosides alleviate colitis, likely by regulating the expression of genes associated with stemness and modulating the tricarboxylic acid cycle and amino acid metabolism, in a DSS-induced colitis mouse model.

Keywords Gypenosides, Colitis, Metabolomics, Transcriptome, Stemness

Ulcerative colitis (UC) is a chronic and recurrent autoimmune disease. The incidence of UC has been increasing globally over the past few decades, particularly in newly industrialized countries in Asia, such as China and India[1]. Although the exact cause of UC remains unclear, several studies indicate that various factors play important roles in its pathogenesis. These factors include genetics, environmental exposures, immune dysregulation, alterations in the gut microbiota, barrier dysfunction, and endoplasmic reticulum stress[2]. 5-Aminosalicylic acid drugs, steroids, immunosuppressants, immunomodulators, biologics, and surgery are the most widely used treatments for UC[3]. Although effective means of treatment have been applied in controlling UC, the management of UC has remained a challenge until now. Further studies are needed to discover new therapeutic drugs and preventive strategies.

Traditional Chinese Medicine (TCM) is recognized for its multitarget approach and low toxicity, making it increasingly important in research on the prevention and treatment of UC. Traditionally, *Gynostemma*

[1]Department of Gastroenterology, The First Affiliated Hospital, Hengyang Medical School, University of South China, Hengyang 421001, Hunan, China. [2]Department of Geriatrics Ward 2, The First Hospital of Lanzhou University, Lanzhou 730000, Gansu, China. [3]Yuan Yang, Xinyuan Li and Fan Huang have contributed equally to this work. ✉email: zbss1229@163.com; 543906753@qq.com; 360680725@qq.com

pentaphyllum was prepared as a tea and valued for its delightful flavor and weight loss benefits. Researchers have further identified numerous bioactive compounds in *Gynostemma pentaphyllum*, including saponins (gypenosides), polysaccharides, flavonoids, and phytosterols. Studies indicate that the active components in *Gynostemma pentaphyllum* significantly inhibit the production and release of inflammatory mediators, thereby reducing intestinal inflammation. For example, one study demonstrated that *Gynostemma pentaphyllum* extract alleviates colitis symptoms in a rat model through inhibiting the nuclear factor-kappa B (NF-κB) signalling pathway. The herb has immunomodulatory effects, balancing the immune system and reducing autoimmune damage to the intestines[4]. Gynostemma pentaphyllum can also regulate the functions of T cells and B cells, promoting immune responses in vivo[5]. Moreover, gypenosides, the primary active components of *Gynostemma pentaphyllum*, have been reported to have significant anti-inflammatory and antioxidant effects[6–11]. Previous studies have demonstrated that gypenosides are capable of reducing oxidative stress damage to the intestines, and alleviating intestinal inflammation by inhibiting the release of inflammatory mediators, thereby suppressing inflammatory signalling pathways[12]. In terms of their anti-inflammatory and antioxidant effects, gypenosides show multifaceted potential in the treatment of intestinal diseases. Several studies have further demonstrated that it enhances intestinal barrier function and reduces intestinal permeability[13]. However, the potential therapeutic effects of gypenosides on UC have not been reported. Therefore, we aimed to evaluate the potential impact of gypenosides on UC and the underlying mechanisms in this study.

A series of studies have reported that high-throughput transcriptomics and metabolomics are effective approaches for elucidating the mechanisms of TCM active compounds[14]. Transcriptomic analysis reveals the relationships between gene expression patterns and cellular functions, biological processes, and disease mechanisms, and has been widely used to identify TCM-affected genes[15,16].These genes directly participate in or regulate metabolic pathways, thereby influencing the production of and changes in metabolites. Metabolites can also influence gene expression through feedback mechanisms. When TCM is effective, integrated analysis helps establish causal networks from gene expression to metabolite production, revealing the underlying biological mechanisms[17]. In this study, we created an animal model of UC with dextran sulfate sodium (DSS) to explore the anti-UC effect of gypenosides. Additionally, we used a multiomics approach to screen potential targets and explore the mechanism of gypenosides. To confirm the relevant mechanism, we detected the expression of candidate genes via molecular methods. In conclusion, we investigated the anti-UC effects of gypenosides and the underlying mechanisms.

Methods

Animals

Six-to eight-week-old male C57BL/6J mice were purchased from Hunan SJA Laboratory Animal Co., Ltd. The mice were housed in a specific pathogen-free (SPF) facility at the Animal Center of South China University. The environmental conditions were maintained at a temperature of 22 ± 2 °C and a humidity of 55 ± 5%, with a 12 h light/dark cycle. All the mice were acclimated for 1 week prior to the experiments. All procedures will be approved by the First Hospital of South China University (2023LL0908001), in line with the Guide for ARRIVE to decrease animal number and suffering as much as possible. All methods were carried out in accordance with relevant regulations and ARRIVE guidelines.

Construction of UC animal models

C57BL/6J mice were first stratified into blocks of three based on their initial body weight to ensure homogeneity within blocks. Then mice were randomly divided into three groups: the control (NC) group, the model (DSS) group, and the gypenosides (GP) group, with 10 mice in each group. Except for those in the control group, all the mice were administered 3.0% DSS for 7 days to induce acute colitis. The mice in the gypenosides (GP) group were gavaged with a 400 mg/kg gypenosides solution until the DSS treatment was stopped. During the modeling period, monitoring of body weight, stool consistency, and the presence of occult or gross blood in the stool was conducted to assess the progression of colitis[18].

Histopathological validation

On the 8th day of the experiment, the mice were anaesthetized prior to sacrifice using carbon dioxide. The length of each colon was measured. Colon tissues were harvested, fixed in 10% neutral-buffered formalin, embedded in paraffin, and sectioned. The tissue sections were stained with haematoxylin and eosin (H&E) to evaluate histopathological changes. Histopathological evaluation were performed via a standard scoring system to quantify the severity of inflammation and tissue damage[19].

Enzyme-linked immunosorbent assay (ELISA)

The levels of TNF-α, and IL-6 in colon tissues were quantified using ELISA kits following the manufacturer's protocols. The concentrations in the colonic tissues were normalized using a bicinchoninic acid (BCA) assay.

Transcriptomic sequencing

Total RNA was extracted from colon tissues using TRIzol reagent following the manufacturer's protocol. The RNA quality and concentration were assessed using a NanoDrop spectrophotometer and Agilent Bioanalyzer. RNA-Seq libraries were prepared using the Illumina TruSeq RNA Sample Preparation Kit. After library construction, PCR amplification was employed to enrich library fragments, selecting a library size of approximately 450 bp. The library was then quality checked via an Agilent 2100 Bioanalyzer, and both the total and effective concentrations of the library were measured. The raw sequencing data underwent quality control using FastQC, and then were filtered using HISAT2 to remove low-quality sequences. These high-quality sequences were then aligned to the reference genome of the species. The remaining high-quality sequences were then aligned to the reference

genome of the species. This alignment allows us to determine the genomic position of each sequence and calculate the expression level of each gene. Differentially expressed genes (DEGs) were subsequently identified via DESeq2 with the criteria of |log2-fold change| > 1 and an adjusted p value < 0.05.

Gene ontology (GO) and kyoto encylcopedia of genes and genomes (KEGG) pathway enrichment analysis

All identified genes were subjected to KEGG pathway and GO enrichment analyses via the "clusterProfiler" and "topGO", respectively, with annotations from "org.Mm.eg.db" in R. The significance thresholds were set at a p value < 0.01 and a q-value < 0.05.

Pathway impact diagram

A pathway impact diagram combines the centrality of metabolites within a network and pathway enrichment results. It calculates the sum of importance measures for each matched metabolite, then divides this sum by the total importance measures of all metabolites within each pathway. For the importance measures, we utilized both betweenness centrality and out-degree centrality.

Immunohistochemical validation

Paraffin-embedded colon sections were deparaffinized, rehydrated, and subjected to antigen retrieval. The sections were incubated with the primary antibody at 4 °C overnight. After the samples were washed, they were incubated with an HRP-conjugated secondary antibody at room temperature for 1 h. Freshly prepared DAB substrate solution was added for colour development. The slides were counterstained with haematoxylin and examined via a light microscope.

Metabolomic analysis

Blood samples were delivered to Bioprofile for the metabolomics analysis. Blood samples were collected by enucleating the eyes via sterile surgical tweezers. After allowing the blood to sit for 30 min, it was centrifuged (3500 rpm, 4 °C, 30 min) to obtain the serum, which was then stored at -80 °C for future use. Metabolomic analysis was conducted using a UPLC-ESI-Q-Orbitrap-MS system. QC samples were used to equilibrate the chromatography-mass spectrometry system, monitor instrument performance, and assess overall system stability throughout the experimental process. For liquid chromatography, samples were separated on an Acquity UPLC column from Waters. The flow rate was maintained at 0.3 mL/min with mobile phase A (0.1% formic acid in water) and mobile phase B (100% acetonitrile). The gradient program was as follows: 0% B for 2 min, increased to 48% B over 4 min, ramped up to 100% B over 4 min, held at 100% B for 2 min, decreased to 0% B in 0.1 min, and then re-equilibrated for 3 min. Mass spectrometry data were acquired in both positive and negative modes using electrospray ionization (ESI). The HESI source conditions were: spray voltage at 3.8 kV (positive) and 3.2 kV (negative); capillary temperature at 320 °C; sheath gas flow rate at 30 ARB; auxiliary gas flow rate at 5 ARB; probe heater temperature at 350 °C; and S-lens RF level at 50. The full MS scan range was 70–1050 m/z, with a resolution of 70,000 at m/z 200 for full MS scans and 17,500 at m/z 200 for MS/MS scans. The maximum injection time was set to 100 ms for MS and 50 ms for MS/MS. The MS2 isolation window was 2 m/z, with stepped normalized collision energies of 20, 30, and 40. Processed data underwent rigorous quality control and transformation. Metabolic features exhibiting > 50% missingness within any experimental group were excluded, followed by independent total peak area normalization of positive and negative ionization mode datasets. Subsequently, integrated cross-mode features were subjected to multivariate pattern recognition using Python. The variable importance for the projection (VIP) scores obtained from the OPLS-DA model were used to assess the impact and explanatory power of each metabolite's expression pattern in distinguishing between different sample groups. This approach helps to identify biologically significant differentially abundant metabolites. One-way ANOVA test was used to analyse the significance of metabolites across multiple groups. Metabolites with a p value less than 0.05 and an OPLS-DA VIP score greater than 1 were considered statistically significant. The pathway impact plot is a combination of the center of the metabolite network and pathway enrichment results. The sum of importance measures for each matching metabolite is calculated and then divided by the sum of importance measures for all metabolites with in each pathway. We used betweenness centrality and out degree centrality to measure importance.

Integrated transcriptomic and metabolomic analysis

Integrated analysis of transcriptomic and metabolomic data were performed to identify correlations between gene expression and metabolite levels. Correlation analysis refers to the examination of two or more correlated variables to measure the degree of association between them. The Spearman correlation coefficient can be used to assess the relationships between species diversity and metabolites in environmental samples. In this study, the Spearman correlation method was used to calculate the correlation coefficients between significantly different metabolites and significantly different genes in R (version 4.0.5). To streamline the data for visualization, we ranked the elements on the basis of the absolute value of their correlation coefficients between the two omics methods and selected the top 60 elements. These elements were used for subsequent correlation coefficient matrix heatmaps, hierarchical clustering heatmaps, and correlation network diagrams.

Statistical analysis

The data are presented as the means ± standard deviation (SDs). Comparisons between groups were statistically analysed using Student's t-test or ANOVA (post-test: Tukey), depending on the experimental design. Statistical significance was set at a p value < 0.05. All analyses were performed using GraphPad Prism or SPSS software.

Results

Gypenosides alleviate symptoms in DSS-induced UC model mice

To evaluate the therapeutic effect of gypenosides on UC, DSS-induced UC model mice were treated with gypenosides(Fig. 1A). Compared with their initial body weights, the body weights of the mice treated with gypenosides were greater (Fig. 1B), and the disease activity indexes (DAIs) were lower (Fig. 1C). Treatment with gypenosides also led to a statistically significant trend towards increased colon length (Fig. 2A). H&E stained sections revealed that gypenosides restored the morphology and architecture of the colonic villi damaged by DSS (Fig. 2B). The pathological state of the GP group significantly improvement. The expression levels of colon inflammatory factors in the GP group were significantly lower than those in the DSS group (Fig. 2C). Overall, these results demonstrate that gypenosides treatment can alleviate symptoms in a DSS-induced UC mouse model.

Effects of gypenosides on the transcriptome of the colon

To differentially expressed genes between the two groups, a volcano plot was generated. A total of 2099 DEGs were identified between the NC and DSS groups, with 1243 upregulated and 856 downregulated genes (Fig. 3A). A total of 356 DEGs were identified between the DSS and GP groups, with 254 upregulated and 102 downregulated genes (Fig. 3B). A total of 1657 DEGs were identified between the DSS and GP groups, with 1081 upregulated genes and 576 downregulated genes (Fig. 3C). Venn diagrams show the shared and unique genes among the

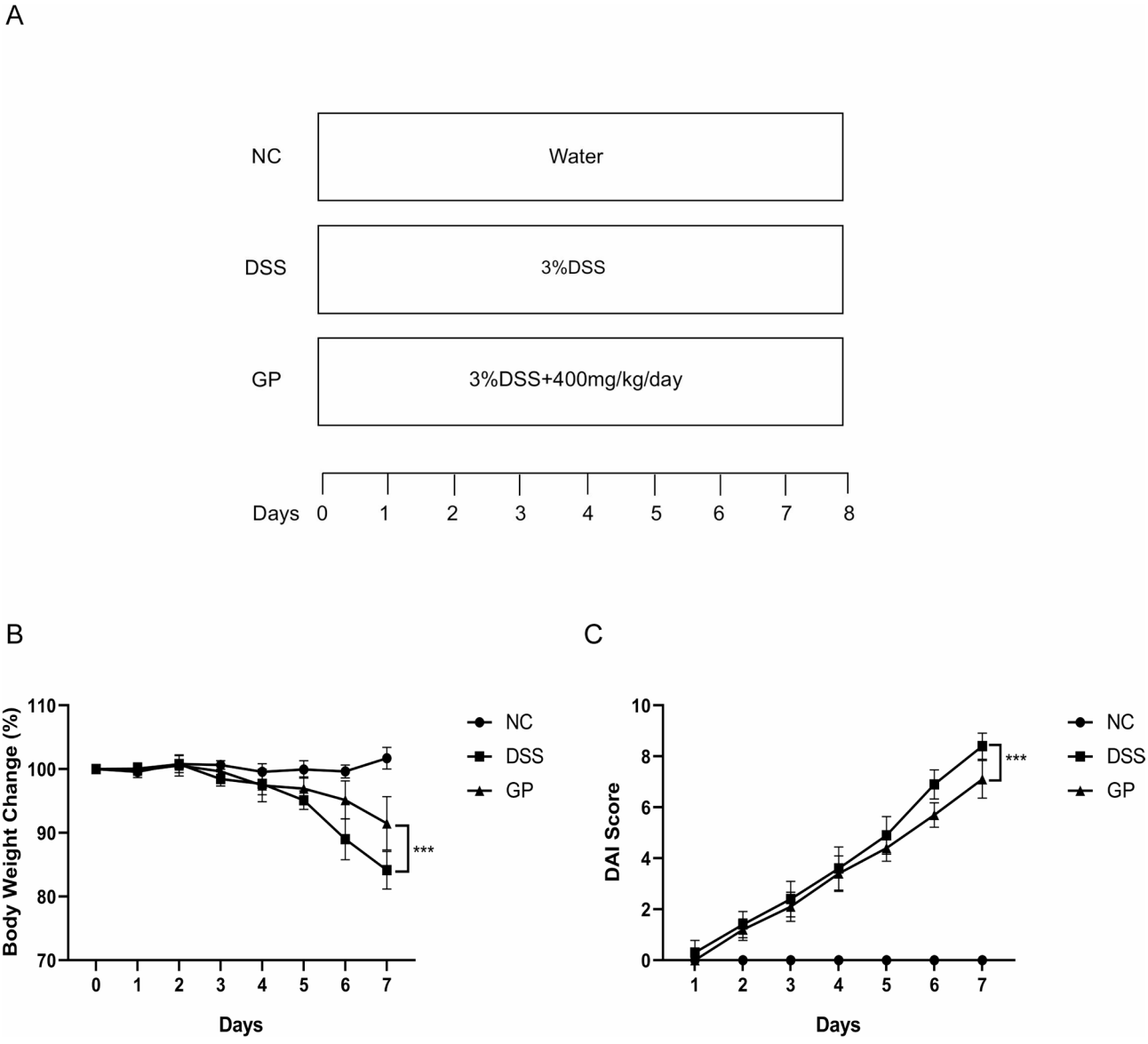

Fig. 1. Gypenosidess alleviated the progression of UC in mice with DSS-induced colitis. (**A**) Experimental design flow. Changes in body weight (**B**) and the DAI (**C**) were monitored over 7 days of DSS induction. Compared with the DSS group, $^{*}P<0.05$, $^{**}P<0.01$, $^{***}P<0.001$.

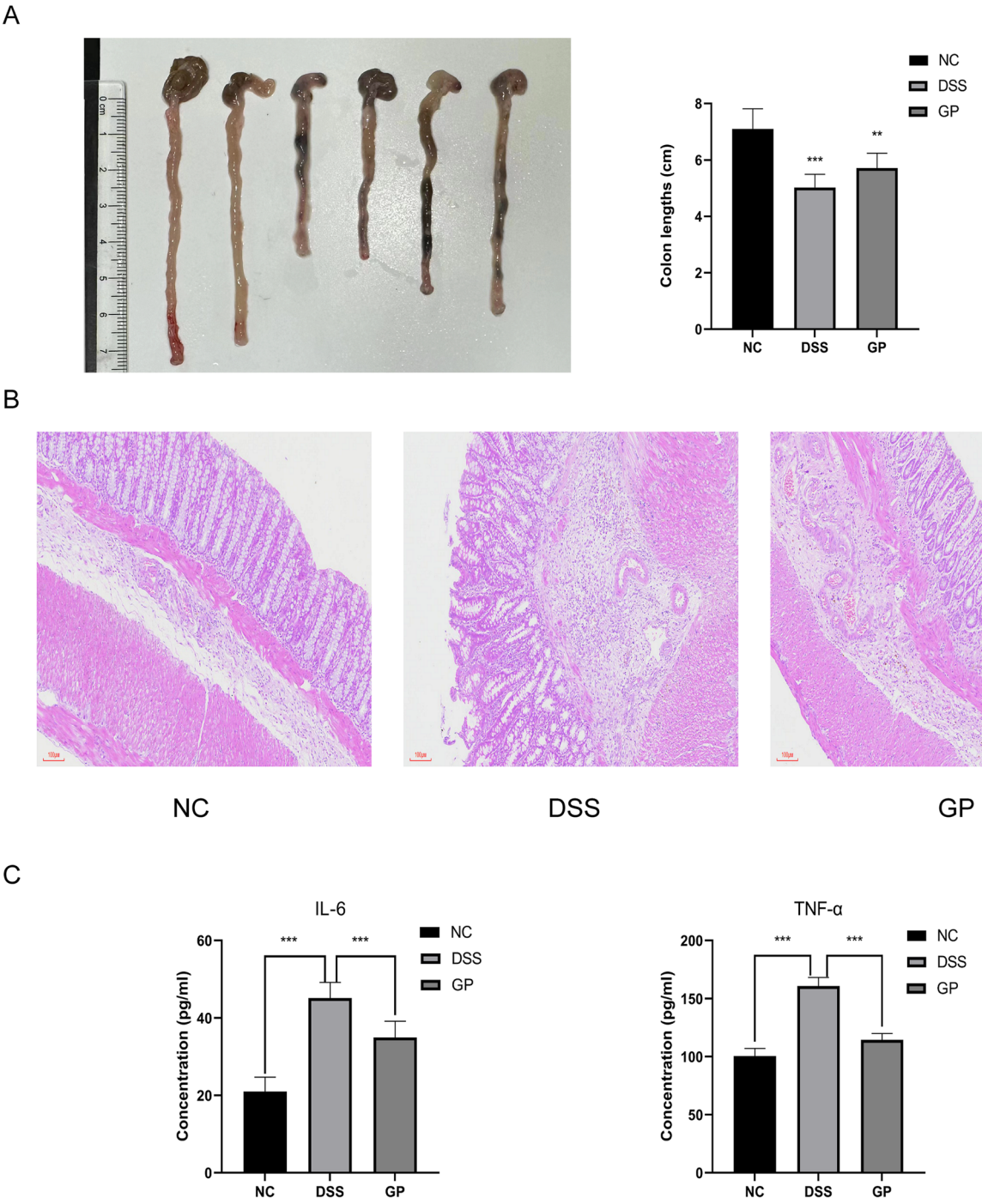

Fig. 2. Gypenosidess slowed the progression of UC in mice with DSS-induced colitis. (**A**) Images and lengths of colons from the three experimental groups. (**B**) Representative H&E staining. (**C**) Levels of IL-6 and TNF-α. Compared with the DSS group, $^{*}P<0.05$, $^{**}P<0.01$, $^{***}P<0.001$.

three groups (Fig. 3D). The DEGs were predominantly associated with signal transduction and the immune system, such as the response to external stimuli, the inflammatory response, the defence response, immune system processes, the immune response, the response to other organisms, the response to external biotic stimuli, the regulation of immune system processes, the response to biotic stimuli, and the regulation of the response to external stimuli (Fig. 4A–D). These findings suggest that gypenosides may exert their anti-UC effects primarily through immune regulation, cell signal transduction, stress response, and adaptation mechanisms.

Gypenosides increase amino acid metabolite levels in DSS-induced UC model mice

OPLS-DA was performed on all metabolic profiles to study the overall metabolic changes in each group of mice. The three-dimensional results show that the samples were clearly distributed in three regions according

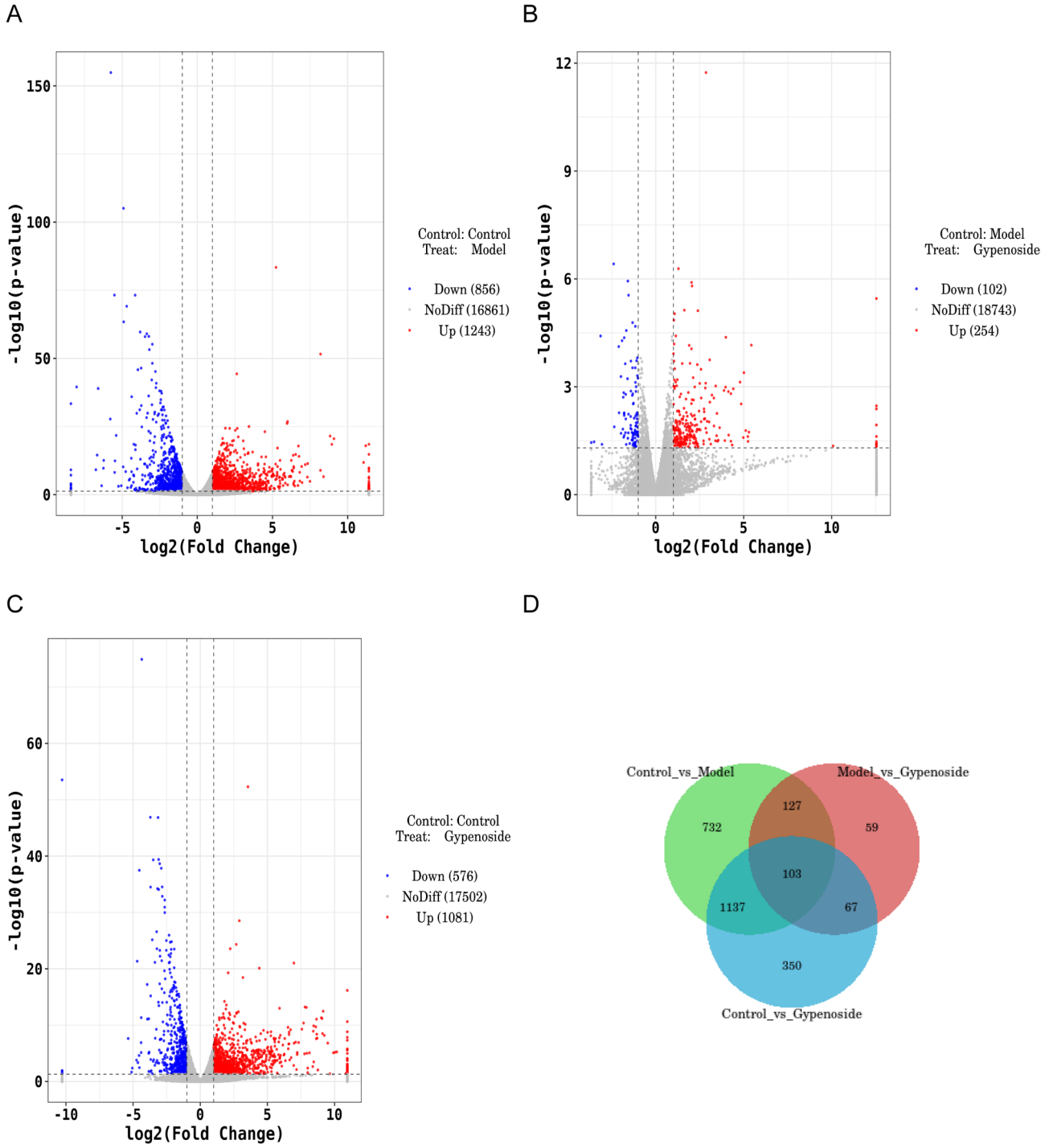

Fig. 3. Effects of gypenosidess treatment on intestinal transcript levels in DSS-induced colitis model mice. Differentially abundant transcripts were compared between the NC group and the DSS group (**A**), the DSS group and the GP group (**B**), and the NC group and the GP group (**C**), with differences defined by a fold change ≥ 1.5 and a *P* value < 0.05. (**D** Venn diagram showing differentially abundant transcripts among the three groups ($n = 10$).

to the processing method (Figure S1). Most of the changes were observed between the DSS and the NC group (Fig. 5A), as well as the comparison between the GP group and the model group (Fig. 5B), indicating that both UC modelling and gypenosides treatment significantly altered the metabolic components in mouse serum. All replicates of each processed organism were clustered together and significantly separated from the other samples. Using the projection variable importance (VIP) of the OPLS-DA model, as well as univariate analysis (T-test *P* value) and multiple change (FC), we determined the differentially abundant metabolites in the serum of the DSS group compared with the NC group. The screening criteria were VIP > 1, FC > 1.5 or FC < 1/1.5, and a *P*

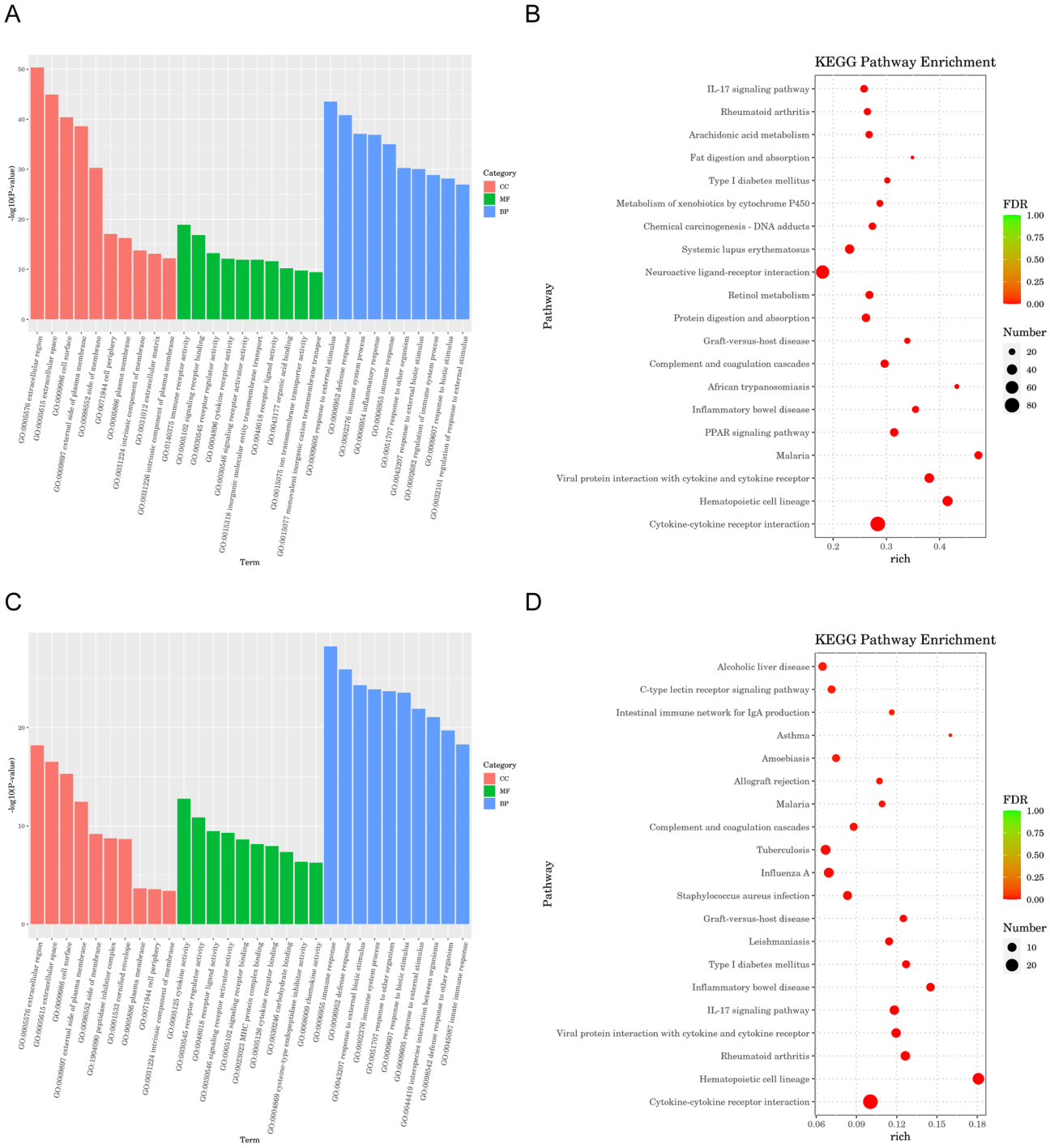

Fig. 4. GO and KEGG enrichment analyses. Histogram of the GO analysis results for (**A**) the NC group and the DSS group and (**C**) the DSS group and the GP group. Bubble plot of the KEGG analysis results for (**B**) the NC group and the DSS group and (**D**) the DSS group and the GP group.

value < 0.05. We generated a chord diagram, and further pathway impact analysis revealed that the differentially abundant metabolites were associated with amino acid biosynthesis, aminoacyl tRNA synthesis, arginine biosynthesis, and glutamate metabolism (Fig. 5C, D). Furthermore, a total of 245 different metabolites were identified among the three groups. The number of differentially abundant metabolites between the DSS group and the NC group, as well as between the GP group and the DSS group, was 249 and 86, respectively (Fig. 6A, B). Pathway analysis suggested that saponins from *Gynostemma pentaphyllum* may alleviate inflammatory symptoms by regulating amino acid metabolism pathways (Fig. 6C-D).

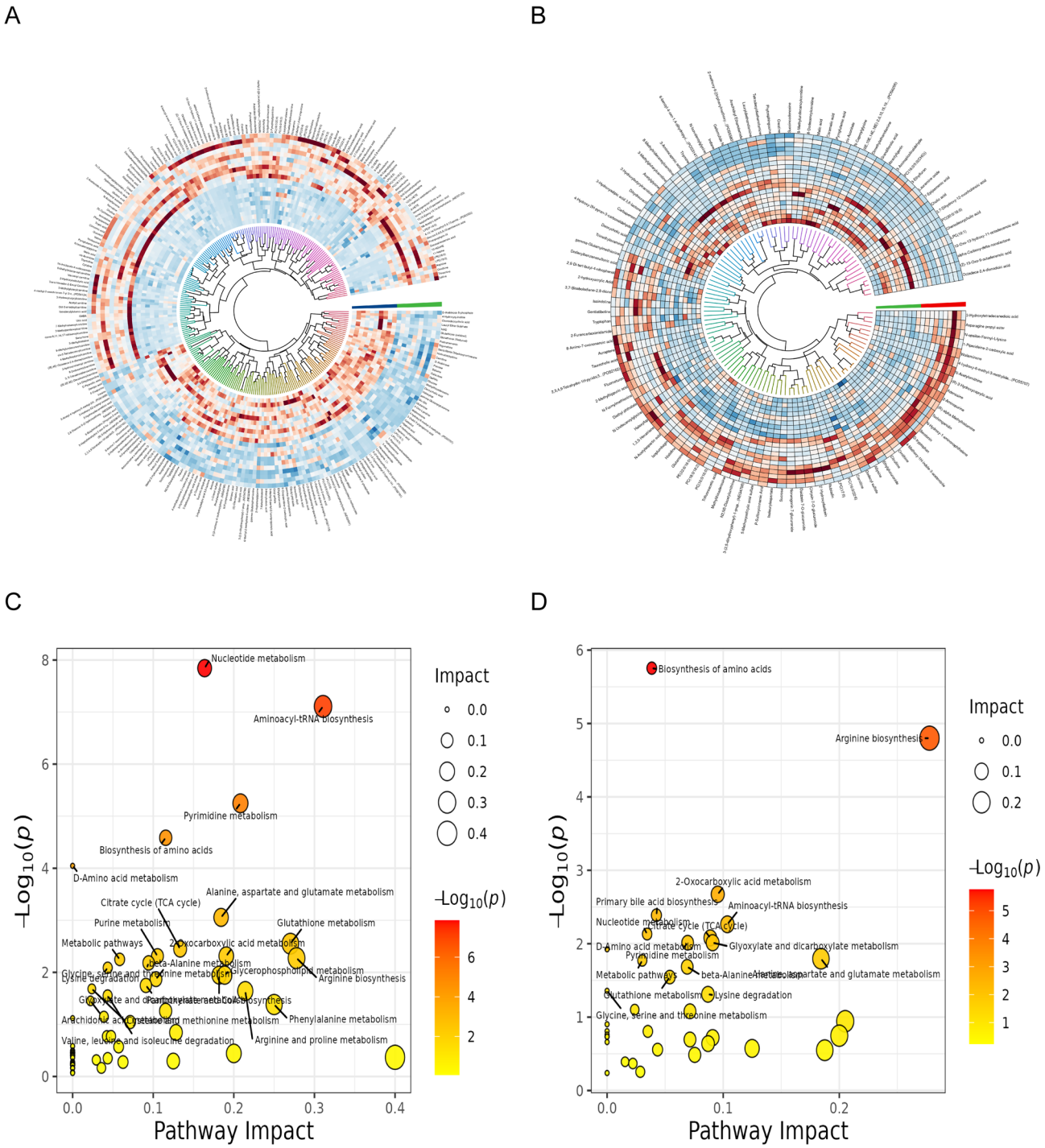

Fig. 5. Effect of gypenosidess on intestinal metabolism in DSS-induced colitis model mice. Differentially abundant metabolites between the NC group and the DSS group (**A**), the DSS group and the GP group (**B**), the NC group and the GP group (**C**). The criteria for determining differences were a fold change ≥ 1.5 and a p value < 0.05. Pathway impact analysis between the NC group and the DSS group (**C**), and between the DSS group and the GP group (**D**).

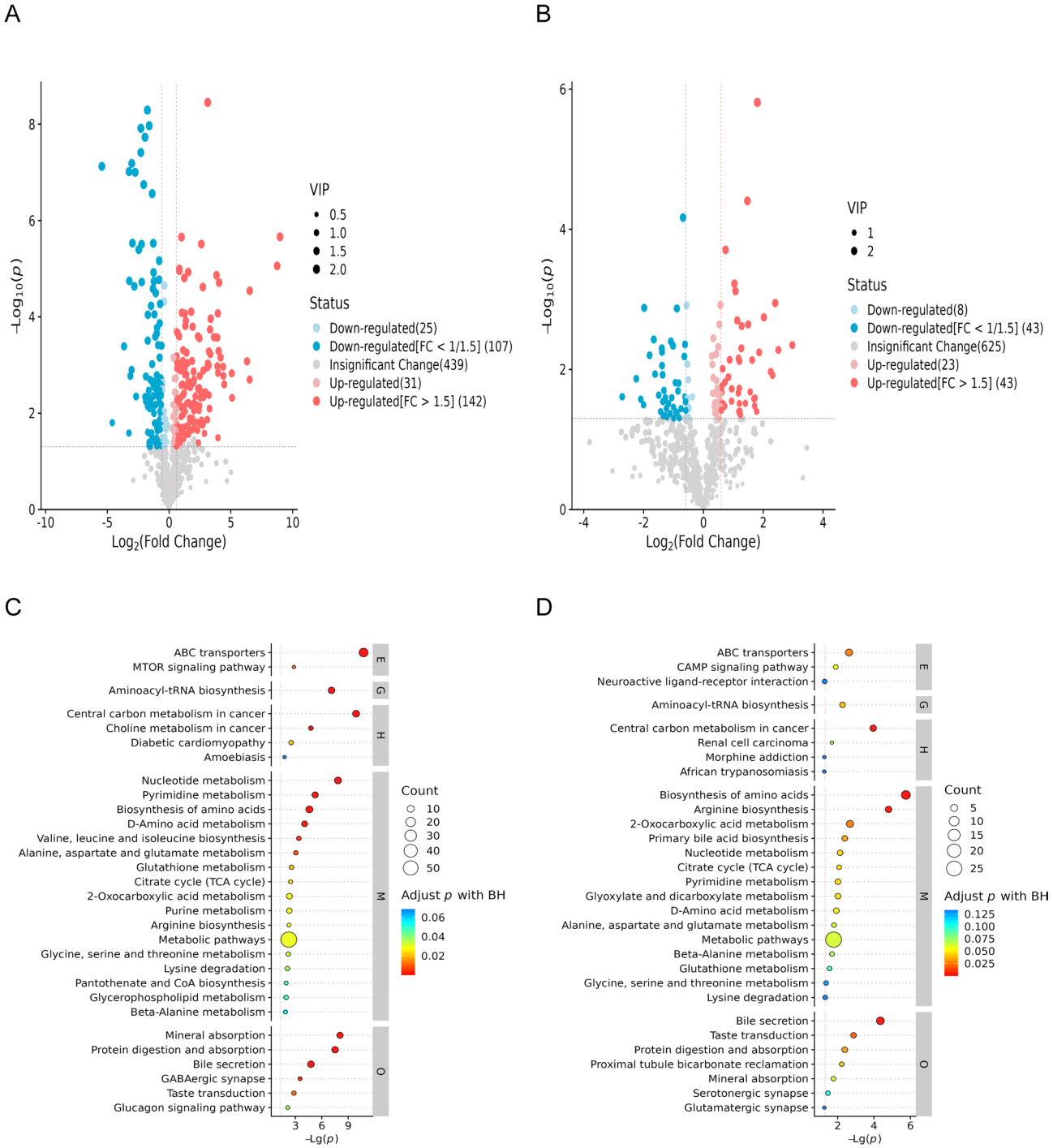

Fig. 6. Changes in intestinal metabolism caused by gypenosides treatment. Volcano plot of metabolism between the NC group and the DSS group (**A**), and between the DSS group and the GP group (**B**). KEGG analysis revealed potential pathways associated with metabolites involved in regulation between the NC group and the DSS group (**C**), and between the DSS group and the GP group (**D**).

Immunohistochemical analysis

The highly expressed differentially expressed genes are listed in Table 1. To confirm the reliability of the RNA sequencing results, immunohistochemistry was conducted. Compared with those in the NC group mice, the protein expression levels of Ascl2 and Lgr5 were significantly lower in the colons of the DSS group mice, and gypenosides administration restored the altered gene expression levels to levels similar to those in the NC group.

Lgr5 and Ascl2 are key markers and regulators of intestinal stem cells, and play crucial roles in the maintenance and regeneration of the intestinal epithelium. Our transcriptome sequencing analysis revealed that Lgr5 and Ascl2 were among the top 20 DEGs. Therefore, we selected Lgr5 and Ascl2 as differential genes for

Table 1. The differentially expressed genes in different groups.

gene_id	Model_vs_Gypenoside_de	Model_vs_Gypenoside_log2fc	Model_vs_Gypenoside_pval	Control_vs_Model_de	Control_vs_Model_log2fc
ENSMUSG00000025082	Up	2.032565173	1.25604E-06	Down	−1.177798237
ENSMUSG00000023886	Up	1.074034671	9.33692E-06	Down	−1.317618818
ENSMUSG00000070304	Up	1.016385679	0.000968225	Down	−1.21956408
ENSMUSG00000033967	Up	1.896671683	7.04983E-05	Down	−1.418756673
ENSMUSG00000022018	Up	1.286232078	5.1858E-07	Down	−2.31953627
ENSMUSG00000029832	Up	1.073536239	0.000980464	Down	−2.254324346
ENSMUSG00000074480	Up	1.142611056	3.84725E-05	Down	−1.281798435
ENSMUSG00000020140	Up	2.394806268	7.63253E-06	Down	−2.75168487
ENSMUSG00000067599	Down	−1.549039945	2.84099E-06	Up	2.182550553
ENSMUSG00000030173	Down	−1.605149914	0.000595382	Up	2.367735049
ENSMUSG00000023132	Down	−1.415938029	0.000192307	Up	2.322406668
ENSMUSG00000017724	Up	2.063394385	1.57123E-06	Down	−3.359791928
ENSMUSG00000047517	Down	−1.043697117	0.000491369	Up	3.166850419
ENSMUSG00000071553	Up	2.12609418	0.000557254	Down	−1.874963419
ENSMUSG00000000318	Down	−1.092390374	0.00018927	Up	1.752234909
ENSMUSG00000025163	Down	−1.793552743	4.3183E-05	Up	1.788178623
ENSMUSG00000062082	Down	−1.114847053	0.000993498	Up	1.324594719
ENSMUSG00000038304	Down	−1.317504254	1.64095E-05	Up	1.379448006
ENSMUSG00000009185	Down	−1.162650035	0.000296416	Up	1.313340437
ENSMUSG00000009248	Up	1.627538099	7.39297E-06	Down	-3.039407405
ENSMUSG00000033576	Down	−1.321414348	0.00029605	Up	3.310710508
ENSMUSG00000021214	Down	−1.982937531	0.000519973	Up	5.337297535
ENSMUSG00000053399	Down	−3.139668325	3.86652E-05	Up	2.808715599
gene_id	**Control_vs_Model_pval**	**Control_vs_Gypenoside_de**	**Control_vs_Gypenoside_log2fc**	**Control_vs_Gypenoside_pval**	
ENSMUSG00000025082	0.001559947	–	0.857028713	0.032169303	
ENSMUSG00000023886	2.57316E-12	–	−0.239857515	0.239276579	
ENSMUSG00000070304	4.75987E-08	–	−0.203385643	0.384166069	
ENSMUSG00000033967	0.000278784	–	0.487436651	0.116502854	
ENSMUSG00000022018	4.99616E-30	Down	−1.029214931	1.01677E-05	
ENSMUSG00000029832	6.14286E-22	Down	−1.177970938	2.48513E-05	
ENSMUSG00000074480	6.76732E-09	–	-0.136410137	0.642423757	
ENSMUSG00000020140	5.3495E-40	–	−0.357418938	0.046726629	
ENSMUSG00000067599	5.02756E-19	–	0.628550174	0.331722605	
ENSMUSG00000030173	1.21963E-07	–	0.761481526	0.3728313	
ENSMUSG00000023132	2.04951E-20	–	0.900390529	0.22605681	
ENSMUSG00000017724	9.42112E-60	Down	−1.288101348	1.06015E-08	
ENSMUSG00000047517	2.19788E-15	Up	2.126222078	4.93154E-05	
ENSMUSG00000071553	4.01275E-09	–	0.257604088	0.518340208	
ENSMUSG00000000318	1.40318E-10	–	0.659585945	0.036641544	
ENSMUSG00000025163	7.2767E-07	–	−0.010669948	0.974912998	
Continued					

gene_id	Control_vs_Model_pval	Control_vs_Gypenoside_de	Control_vs_Gypenoside_log2fc	Control_vs_Gypenoside_pval	
ENSMUSG00000062082	3.05705E-07	–	0.20762448	0.56807924	
ENSMUSG00000038304	4.1822E-10	–	0.060125304	0.81600711	
ENSMUSG00000009185	3.83013E-05	–	0.149856188	0.467550608	
ENSMUSG00000009248	4.77142E-13	Down	−1.412030307	3.94524E-05	
ENSMUSG00000033576	9.50761E-12	Up	1.991244578	1.87373E-07	
ENSMUSG00000021214	4.76818E-11	Up	3.356993285	0.000159069	
ENSMUSG00000053399	8.93362E-05	–	−0.338582615	0.734889128	
gene_id	**Chromosome**	**Start site**	**End site**	**Direction**	**Length**
ENSMUSG00000025082	19	56862681	56900510	+	4049
ENSMUSG00000023886	17	14499768	14625052	+	6951
ENSMUSG00000070304	9	45029080	45041368	+	4656
ENSMUSG00000033967	7	12661343	12664999	+	3239
ENSMUSG00000022018	14	79526196	79539085	–	918
ENSMUSG00000029832	6	51409650	51435748	+	2973
ENSMUSG00000074480	3	88439702	88448703	+	5778
ENSMUSG00000020140	10	115286216	115423685	–	10264
ENSMUSG00000067599	6	130195568	130210285	–	1265
ENSMUSG00000030173	6	129875959	129894613	–	1398
ENSMUSG00000023132	13	113230359	113237515	–	1006
ENSMUSG00000017724	11	101660568	101676197	–	3104
ENSMUSG00000047517	7	130633776	130723357	+	7718
ENSMUSG00000071553	6	30541581	30564475	+	3212
ENSMUSG00000000318	11	70047023	70061660	+	2899
ENSMUSG00000025163	11	120927573	120930244	–	1133
ENSMUSG00000062082	16	44632096	44659513	+	2045
ENSMUSG00000038304	3	96706079	96736667	–	2642
ENSMUSG00000009185	11	82006011	82007625	+	511
ENSMUSG00000009248	7	142520566	142523001	–	1623
ENSMUSG00000033576	15	76928929	76941306	+	4498
ENSMUSG00000021214	13	4182614	4200653	–	1207
ENSMUSG00000053399	8	114423758	114575370	–	10178

gene_id	Name	GO	KEGG	EC
ENSMUSG00000025082	Vwa2	GO:0005509;GO:0005576;GO:0005604;GO:0005615;GO:0007161;GO:0031012;GO:0042802;GO:0046626;GO:0062023	K24508	–
ENSMUSG00000023886	Smoc2	GO:0005509;GO:0005515;GO:0005539;GO:0005576;GO:0005604;GO:0005614;GO:0005615;GO:0008201;GO:0010595;GO:0010811;GO:0030198;GO:0031012;GO:0035470;GO:00 45743;GO:0045766;GO:0045931;GO:0046872;GO:0050840;GO:0062023;GO:0071944;GO:1900748;GO:2000573;GO:2001028	K24354	–
ENSMUSG00000070304	Scn2b	GO:0001518;GO:0005244;GO:0005248;GO:0005272;GO:0005886;GO:0006811;GO:0006814;GO:0007399;GO:0009408;GO:0010467;GO:0016020;GO:0016021;GO:0017080;GO:00 30315;GO:0034765;GO:0035725;GO:0046684;GO:0060048;GO:0060371;GO:0061337;GO:0086002;GO:0086006;GO:0086012;GO:0086091;GO:0098915;GO:1902282;GO:2000649	K04846	–
ENSMUSG00000033967	Rnf225	GO:0005575;GO:0016020;GO:0016021;GO:0016567;GO:0046872;GO:0061630	–	–
ENSMUSG00000022018	Rgcc	GO:0000082;GO:0001100;GO:0001818;GO:0001819;GO:0001937;GO:0003331;GO:0005515;GO:0005634;GO:0005654;GO:0005730;GO:0005737;GO:0005813;GO:0005815;GO:00 05856;GO:0006956;GO:0007049;GO:0008285;GO:0010628;GO:0010718;GO:0016525;GO:0019901;GO:0030295;GO:0032147;GO:0032967;GO:0043537;GO:0045737;GO:0045840;G- O:0045944;GO:0051091;GO:0051496;GO:0051726;GO:0070412;GO:0071456;GO:0072537;GO:0090272;GO:1900087;GO:1901203;GO:1901991;GO:2000048;GO:2000353;GO:2000573	K26108	–
ENSMUSG00000029832	Nfe2l3	GO:0000122;GO:0000978;GO:0000981;GO:0001227;GO:0003677;GO:0003700;GO:0005634;GO:0006355;GO:0006357;GO:0090575	K09040	–
ENSMUSG00000074480	Mex3a	GO:0000932;GO:0003674;GO:0003676;GO:0003723;GO:0005829;GO:0008150;GO:0046872	K15686	EC:2.3.2.27
ENSMUSG00000020140	Lgr5	GO:0001942;GO:0004888;GO:0004930;GO:0005515;GO:0005654;GO:0005794;GO:0005886;GO:0005887;GO:0007165;GO:0007186;GO:0009994;GO:0016020;GO:0016021;GO:00 16500;GO:0032588;GO:0042127;GO:0048839;GO:0090263;GO:2001013	K04308	–
ENSMUSG00000067599	Klra7	GO:0005886;GO:0007155;GO:0009897;GO:0016020;GO:0016021;GO:0030246	K24238	–
ENSMUSG00000030173	Klra5	GO:0005886;GO:0007155;GO:0016020;GO:0016021;GO:0030246	-	–
ENSMUSG00000023132	Gzma	GO:0004252;GO:0005576;GO:0005634;GO:0006508;GO:0008233;GO:0008236;GO:0009617;GO:0016787;GO:0019835;GO:0032078;GO:0042803;GO:0043065;GO:0043392;GO:00 51354;GO:0051603;GO:0070269;GO:0140507;GO:1902483	K01352	EC:3.4.21.78
ENSMUSG00000017724	Etv4	GO:0000978;GO:0000981;GO:0001228;GO:0003677;GO:0003700;GO:0005634;GO:0005694;GO:0005730;GO:0006355;GO:0006357;GO:0006366;GO:0008045;GO:0010628;GO:00 30154;GO:0033600;GO:0043565;GO:0045618;GO:0045893;GO:0045944;GO:0048863;GO:0060444;GO:1990837	K15592	–
ENSMUSG00000047517	Dmbt1	GO:0005044;GO:0005576;GO:0006897;GO:0015031;GO:0016020;GO:0016021;GO:0030154;GO:0110165	K13912	–
ENSMUSG00000071553	Cpa2	GO:0004180;GO:0004181;GO:0005576;GO:0005615;GO:0006508;GO:0008233;GO:0008237;GO:0008270;GO:0016787;GO:0046872	K01298	EC:3.4.17.15
ENSMUSG00000000318	Clec10a	GO:0002248;GO:0009897;GO:0016020;GO:0016021;GO:0030246	K06721	–
ENSMUSG00000025163	Cd7	GO:0002250;GO:0002376;GO:0016020;GO:0016021;GO:0038023;GO:0048873	K06457	–
ENSMUSG00000062082	Cd200r4	GO:0005515;GO:0005886;GO:0009897;GO:0009986;GO:0016020;GO:0016021;GO:0038023;GO:0150077	K21668	–
ENSMUSG00000038304	Cd160	GO:0002250;GO:0002376;GO:0002385;GO:0002729;GO:0002819;GO:0002857;GO:0004888;GO:0005102;GO:0005515;GO:0005576;GO:0005886;GO:0014065;GO:0016020;GO:0016525;GO:0019900;GO:0023024;GO:00 31225;GO:0031295;GO:0032393;GO:0032394;GO:0032397;GO:0032729;GO:0043323;GO:0045087;GO:0045954;GO:0046658;GO:0050829;GO:0050860;GO:1900280;GO:1905675;GO:2000353	K06542	–
ENSMUSG00000009185	Cd8	GO:0002548;GO:0004672;GO:0005125;GO:0005576;GO:0005615;GO:0006816;GO:0006874;GO:0006887;GO:0006935;GO:0006954;GO:0006955;GO:0007165;GO:0007186;GO:0007267;GO:0008009;GO:0008201;GO:00 16004;GO:0030593;GO:0031640;GO:0043547;GO:0044828;GO:0045663;GO:0048020;GO:0048245;GO:0048247;GO:0060326;GO:0061844;GO:0070098;GO:0070374;GO:0071346;GO:0071347;GO:0071356;GO:1901741	K16596	–
ENSMUSG00000009248	Ascl2	GO:0000122;GO:0000977;GO:0000978;GO:0000981;GO:0001227;GO:0001666;GO:0001701;GO:0001890;GO:0003677;GO:0003700;GO:0005634;GO:0005737;GO:0006357;GO:0007399;GO:0007423;GO:0010626;GO:00 30154;GO:0030182;GO:0035019;GO:0043565;GO:0045944;GO:0046983;GO:0050767;GO:0060708;GO:0060712;GO:0070888;GO:0090575;GO:1990837	K09067	–
ENSMUSG00000033576	Apol6	GO:0003674;GO:0005575;GO:0005576;GO:0006869;GO:0008150;GO:0008289;GO:0016020;GO:0016021;GO:0042157	K14480	–
ENSMUSG00000021214	Akr1c18	GO:0001758;GO:0004032;GO:0004033;GO:0004745;GO:0005634;GO:0005737;GO:0005829;GO:0006693;GO:0006709;GO:0007186;GO:0007565;GO:0007567;GO:0008202;GO:00 08284;GO:0010942;GO:0016229;GO:0016488;GO:0016491;GO:0016655;GO:0018636;GO:0032052;GO:0034614;GO:0035410;GO:0042448;GO:0042574;GO:0044597;GO:0044598 ;GO:0045550;GO:0045703;GO:0047006;GO:0047020;GO:0047023;GO:0047086;GO:0047787;GO:0048385;GO:0050810;GO:0051897;GO:0061370;GO:0071276;GO:0071277;GO:00713 72;GO:0071379;GO:0071384;GO:0071394;GO:0071395;GO:0071560;GO:0071799;GO:0097211;GO:1900053;GO:1904322;GO:1990646;GO:2000224;GO:2000353;GO:2000379	K05295	EC:1.1.1.149
ENSMUSG00000053399	Adamts18	GO:0001654;GO:0004222;GO:0005576;GO:0005634;GO:0006508;GO:0008233;GO:0008237;GO:0016787;GO:0030198;GO:0031012;GO:0046872;GO:0090331	K08632	EC:3.4.24.–

gene_id	eggNOG class	eggNOG	Description	Entrez_geneID	UniProtAC
ENSMUSG00000025082	T;D	KOG3544;359SZ;39QPM;3BJ7G;3D121;3JDIS;4889C;4935Y;4Q1GH	von Willebrand factor A domain containing 2 [Source:MGI Symbol;Acc:MGI:2684334]	240675	Q70UZ7;Q8CE01
ENSMUSG00000023886	S	KOG4578;35EXC;39SIX;3BCPZ;3CUPY;3J4AW;48APV;4955M;4Q3PM	SPARC related modular calcium binding 2 [Source:MGI Symbol;Acc:MGI:1929881]	64074	Q8CD91
ENSMUSG00000070304	T;P	2R29H;35KKE;38MC8;3BEZ2;3D0AF;3J5SH;488K0;495QK;4PY65	sodium channel, voltage-gated, type II, beta [Source:MGI Symbol;Acc:MGI:106921]	72821	Q56A07;Q1MXF8
ENSMUSG00000033967	O	KOG2177;35FJQ;3A7QW;3BTBD;3D4C1;3J9QG;486K9;497W0;4Q60G	ring finger protein 225 [Source:MGI Symbol;Acc:MGI:1924198]	381845	Q9D7D1
ENSMUSG00000022018	S;K	2S1UB;35PPI;3A3NM;3BRDQ;3D8HJ;3JGF1;48EU0;49BM9;4Q8PZ	regulator of cell cycle [Source:MGI Symbol;Acc:MGI:1913464]	66214	Q9DBX1
ENSMUSG00000029832	K	KOG3863;35MM9;39THC;3BEKZ;3CX4J;3J7TZ;484Z2;48VIJ;4PY0Y	nuclear factor, erythroid derived 2, like 3 [Source:MGI Symbol;Acc:MGI:1339958]	18025	Q9WTM4;Q3UZC1
ENSMUSG00000074480	S;O	KOG2113;3595E;39TJN;3B9BH;3CY96;3J5IM;487YG;496QB;4PZN6	mex3 RNA binding family member A [Source:MGI Symbol;Acc:MGI:1919890]	72640	G3UYU0
ENSMUSG00000020140	T;U	KOG0619;KOG2087;35DDJ;38DRQ;3B9GE;3CSEC;3JBSR;483J8;48Z5S;4PWK2	leucine rich repeat containing G protein coupled receptor 5 [Source:MGI Symbol;Acc:MGI:1341817]	14160	Q9Z1P4
ENSMUSG00000067599	S;T;V	KOG4297;35F8E;3A27M;3BQYM;3D4A6;3J6K3;4887M;4997U;4Q5HW	killer cell lectin-like receptor, subfamily A, member 7 [Source:MGI Symbol;Acc:MGI:101901]	16638	Q60654;F8WJ94
ENSMUSG00000030173	S;T;V	KOG4297;35F8E;3A27M;3BQYM;3D4A6;3J6K3;4887M;4997U;4Q5HW	killer cell lectin-like receptor, subfamily A, member 5 [Source:MGI Symbol;Acc:MGI:101903]	16636	Q60652;Q548A2
ENSMUSG00000023132	O	KOG3627;35AQB;38YQZ;3BDC7;3D50Y;3JDVZ;4874J;48URU;4PW35	granzyme A [Source:MGI Symbol;Acc:MGI:109266]	14938	P11032;Q3U0N0
ENSMUSG00000017724	K	KOG3806;35NXJ;38QW9;3BDHQ;3D2EP;3J4HV;48003;492XC;4Q3KV	ets variant 4 [Source:MGI Symbol;Acc:MGI:99423]	18612	P28322;A6MDC6
ENSMUSG00000047517	S;T;W	2RSDM;39VZN;3BIWA;3E6D2;3JPTT;48RUQ;49N89	deleted in malignant brain tumors 1 [Source:MGI Symbol;Acc:MGI:106210]	12945	Q60997;A0A140LI59
ENSMUSG00000071553	O;E	KOG2650;35CDI;38DUK;3BA6U;3CUQS;3JAWZ;481VD;490AY;4Q6WI	carboxypeptidase A2, pancreatic [Source:MGI Symbol;Acc:MGI:3617840]	232680	Q504N0
ENSMUSG00000000318	S;T;V	KOG4297;35P5C;39YT3;3BMCI;3CVVA;3JAM0;48BF5;48YMK;4Q3MX	C-type lectin domain family 10, member A [Source:MGI Symbol;Acc:MGI:96975]	17312	P49300
ENSMUSG00000025163	S;T	2SD5I;35QB0;3A2S6;3BT2A;3D7HP;3JH0R;48EX6;49BIF;4Q63H	CD7 antigen [Source:MGI Symbol;Acc:MGI:88344]	12516	P50283;Q3U4A8
ENSMUSG00000062082	S;T	2S9IV;35Q1Z;3A2MP;3BR2P;3D278;3J458;488QH;4900F;4Q8NX	CD200 receptor 4 [Source:MGI Symbol;Acc:MGI:3036289]	239849	Q6XJV4
ENSMUSG00000038304	S;T	2RR8D;35PVH;3A0I8;3BQ53;3D6RK;3JGCK;48D6W;49ABT;4Q8T7	CD160 antigen [Source:MGI Symbol;Acc:MGI:1860383]	54215	O88875
ENSMUSG00000009185	–	–	chemokine (C-C motif) ligand 8 [Source:MGI Symbol;Acc:MGI:101878]	20307	Q9Z121;Q149U7
ENSMUSG00000009248	O;K	KOG4029;35VQD;38E2W;3BHUN;3E4DX;3JNJ4;48R3F;49MPF;4Q4C0	achaete-scute family bHLH transcription factor 2 [Source:MGI Symbol;Acc:MGI:96920]	17173	O35885;Q3TJR9
ENSMUSG00000033576	S	2QPNS;35CIJ;3A1BI;3BQ6E;3D1JY;3JF2D;4896G;492TP;4Q54Z	apolipoprotein L 6 [Source:MGI Symbol;Acc:MGI:1919189]	71939	Q3UN08;B7ZC55
ENSMUSG00000021214	S;J;C	KOG1577;35M94;38T1T;3BK9X;3D0AD;3J7EU;4842J;49784;4Q6J6	aldo-keto reductase family 1, member C18 [Source:MGI Symbol;Acc:MGI:2145420]	105349	Q8K023;Q3U538
ENSMUSG00000053399	O	KOG3538;35IXT;38EJ8;3BBR3;3CS90;3JA6A;47Z07;49125;4PUN4	a disintegrin-like and metallopeptidase (reprolysin type) with thrombospondin type 1 motif, 18 [Source:MGI Symbol;Acc:MGI:2442600]	208936	Q4VC17

gene_id	BP	CC	MF	Pathway
ENSMUSG00000025082	GO:0007161//calcium-independent cell-matrix adhesion;GO:0046626//regulation of insulin receptor signaling pathway;	GO:0005576//extracellular region;GO:0005604//basement membrane;GO:0005615//extracellular space;GO:0031012//extracellular matrix;GO:0062023//collagen-containing extracellular matrix;	GO:0005509//calcium ion binding;GO:0042802//identical protein binding;	–
ENSMUSG00000023886	GO:0010595//positive regulation of endothelial cell migration;GO:0010811//positive regulation of cell-substrate adhesion;GO:0030198//extracellular matrix organization;GO:0035470//positive regulation of vascular wound healing;GO:0045743//positive regulation of fibroblast growth factor receptor signaling pathway;GO:0045766//positive regulation of angiogenesis;GO:0045931//positive regulation of mitotic cell cycle;GO:1900748//positive regulation of vascular endothelial growth factor signaling pathway;GO:2000573//positive regulation of DNA biosynthetic process;GO:2001028//positive regulation of endothelial cell chemotaxis;	GO:0005576//extracellular region;GO:0005604//basement membrane;GO:0005614//interstitial matrix;GO:0005615//extracellular space;GO:0031012//extracellular matrix;GO:0062023//collagen-containing extracellular matrix;GO:0071944//cell periphery;	GO:0005509//calcium ion binding;GO:0005515//protein binding;GO:0005539//glycosaminoglycan binding;GO:0008201//heparin binding;GO:0046872//metal ion binding;GO:0050840//extracellular matrix binding;	–

gene_id	BP	CC	MF	Pathway	
ENSMUSG00000070304	GO:0006811//ion transport;GO:0006814//sodium ion transport;GO:0007399//nervous system development;GO:0009408//response to heat;GO:0010467//gene expression;GO:0034765//regulation of ion transmembrane transport;GO:0035725//sodium ion transmembrane transport;GO:0046684//response to pyrethroid;GO:0060048//cardiac muscle contraction;GO:0060371//regulation of atrial cardiac muscle cell membrane depolarization;GO:0061337//cardiac conduction;GO:0086002//cardiac muscle cell action potential involved in contraction;GO:0086012//membrane depolarization during cardiac muscle cell action potential;GO:0086091//regulation of heart rate by cardiac conduction;GO:0098915//membrane repolarization during ventricular cardiac muscle cell action potential;GO:2000649//regulation of sodium ion transmembrane transporter activity;	GO:0001518//voltage-gated sodium channel complex;GO:0005886//plasma membrane;GO:0016020//membrane;GO:0016021//integral component of membrane;GO:0030315//T-tubule;	GO:0005244//voltage-gated ion channel activity;GO:0005248//voltage-gated sodium channel activity;GO:0005272//sodium channel activity;GO:0017080//sodium channel regulator activity;GO:0086006//voltage-gated sodium channel activity involved in cardiac muscle cell action potential;GO:1902282//voltage-gated potassium channel activity involved in ventricular cardiac muscle cell action potential repolarization;	–	
ENSMUSG00000033967	GO:0016567//protein ubiquitination;	GO:0005575//cellular_component;GO:0016020//membrane;GO:0016021//integral component of membrane;	GO:0046872//metal ion binding;GO:0061630//ubiquitin protein ligase activity;	–	

gene_id	BP	CC	MF	Pathway
ENSMUSG00000022018	GO:0000082//G1/S transition of mitotic cell cycle;GO:0001100// negative regulation of exit from mitosis;GO:0001818// negative regulation of cytokine production;GO:0001819// positive regulation of cytokine production;GO:0001937// negative regulation of endothelial cell proliferation;GO:0003331// positive regulation of extracellular matrix constituent secretion;GO:0006956// complement activation;GO:0007049//cell cycle;GO:0008285//negative regulation of cell population proliferation;GO:0010628// positive regulation of gene expression;GO:0010718// positive regulation of epithelial to mesenchymal transition;GO:0016525// negative regulation of angiogenesis;GO:0032147// activation of protein kinase activity;GO:0032967// positive regulation of collagen biosynthetic process;GO:0043537// negative regulation of blood vessel endothelial cell migration;GO:0045737//positive regulation of cyclin-dependent protein serine/threonine kinase activity;GO:0045840// positive regulation of mitotic nuclear division;GO:0045944// positive regulation of transcription by RNA polymerase II;GO:0051091// positive regulation of DNA-binding transcription factor activity;GO:0051496// positive regulation of stress fiber assembly;GO:0051726// regulation of cell cycle;GO:0071456// cellular response to hypoxia;GO:0072537//fibroblast activation;GO:0090272// negative regulation of fibroblast growth factor production;GO:1900087// positive regulation of G1/S transition of mitotic cell cycle;GO:1901203//positive regulation of extracellular matrix assembly;GO:1901991// negative regulation of mitotic cell cycle phase transition;GO:2000048// negative regulation of cell-cell adhesion mediated by cadherin;GO:2000353//positive regulation of endothelial cell apoptotic process;GO:2000573// positive regulation of DNA biosynthetic process;	GO:0005634//nucleus;GO:0005654// nucleoplasm;GO:0005730// nucleolus;GO:0005737// cytoplasm;GO:0005813// centrosome;GO:0005815//microtubule organizing center;GO:0005856// cytoskeleton;	GO:0005515//protein binding;GO:0019901// protein kinase binding;GO:0030295// protein kinase activator activity;GO:0070412//R-SMAD binding;	–
ENSMUSG00000029832	GO:0000122//negative regulation of transcription by RNA polymerase II;GO:0006355//regulation of transcription, DNA-templated;GO:0006357// regulation of transcription by RNA polymerase II;	GO:0005634//nucleus;GO:0090575// RNA polymerase II transcription regulator complex;	GO:0000978// RNA polymerase II cis-regulatory region sequence-specific DNA binding;GO:0000981// DNA-binding transcription factor activity, RNA polymerase II-specific;GO:0001227// DNA-binding transcription repressor activity, RNA polymerase II-specific;GO:0003677// DNA binding;GO:0003700// DNA-binding transcription factor activity;	–

gene_id	BP	CC	MF	Pathway
ENSMUSG00000074480	GO:0008150//biological_process;	GO:0000932//P-body;GO:0005829//cytosol;	GO:0003674//molecular_function;GO:0003676//nucleic acid binding;GO:0003723//RNA binding;GO:0046872//metal ion binding;	–
ENSMUSG00000020140	GO:0001942//hair follicle development;GO:0007165//signal transduction;GO:0007186//G protein-coupled receptor signaling pathway;GO:0009994//oocyte differentiation;GO:0042127//regulation of cell population proliferation;GO:0048839//inner ear development;GO:0090263//positive regulation of canonical Wnt signaling pathway;GO:2001013//epithelial cell proliferation involved in renal tubule morphogenesis;	GO:0005654//nucleoplasm;GO:0005794//Golgi apparatus;GO:0005886//plasma membrane;GO:0005887//integral component of plasma membrane;GO:0016020//membrane;GO:0016021//integral component of membrane;GO:0032588//trans-Golgi network membrane;	GO:0004888//transmembrane signaling receptor activity;GO:0004930//G protein-coupled receptor activity;GO:0005515//protein binding;GO:0016500//protein-hormone receptor activity;	ko04310(Wnt signaling pathway)
ENSMUSG00000067599	GO:0007155//cell adhesion;	GO:0005886//plasma membrane;GO:0009897//external side of plasma membrane;GO:0016020//membrane;GO:0016021//integral component of membrane;	GO:0030246//carbohydrate binding;	ko04650(Natural killer cell mediated cytotoxicity)
ENSMUSG00000030173	GO:0007155//cell adhesion;	GO:0005886//plasma membrane;GO:0016020//membrane;GO:0016021//integral component of membrane;	GO:0030246//carbohydrate binding;	–
ENSMUSG00000023132	GO:0006508//proteolysis;GO:0009617//response to bacterium;GO:0019835//cytolysis;GO:0032078//negative regulation of endodeoxyribonuclease activity;GO:0043065//positive regulation of apoptotic process;GO:0043392//negative regulation of DNA binding;GO:0051354//negative regulation of oxidoreductase activity;GO:0051603//proteolysis involved in cellular protein catabolic process;GO:0070269//pyroptosis;GO:0140507//granzyme-mediated programmed cell death signaling pathway;GO:1902483//cytotoxic T cell pyroptotic process;	GO:0005576//extracellular region;GO:0005634//nucleus;	GO:0004252//serine-type endopeptidase activity;GO:0008233//peptidase activity;GO:0008236//serine-type peptidase activity;GO:0016787//hydrolase activity;GO:0042803//protein homodimerization activity;	ko04080(Neuroactive ligand-receptor interaction)
ENSMUSG00000017724	GO:0006355//regulation of transcription, DNA-templated;GO:0006357//regulation of transcription by RNA polymerase II;GO:0006366//transcription by RNA polymerase II;GO:0008045//motor neuron axon guidance;GO:0010628//positive regulation of gene expression;GO:0030154//cell differentiation;GO:0033600//negative regulation of mammary gland epithelial cell proliferation;GO:0045618//positive regulation of keratinocyte differentiation;GO:0045893//positive regulation of transcription, DNA-templated;GO:0045944//positive regulation of transcription by RNA polymerase II;GO:0048863//stem cell differentiation;GO:0060444//branching involved in mammary gland duct morphogenesis;	GO:0005634//nucleus;GO:0005694//chromosome;GO:0005730//nucleolus;	GO:0000978//RNA polymerase II cis-regulatory region sequence-specific DNA binding;GO:0000981//DNA-binding transcription factor activity, RNA polymerase II-specific;GO:0001228//DNA-binding transcription activator activity, RNA polymerase II-specific;GO:0003677//DNA binding;GO:0003700//DNA-binding transcription factor activity;GO:0043565//sequence-specific DNA binding;GO:1990837//sequence-specific double-stranded DNA binding;	ko05202(Transcriptional misregulation in cancer)

gene_id	BP	CC	MF	Pathway
ENSMUSG00000047517	GO:0006897//endocytosis;GO:0015031//protein transport;GO:0030154//cell differentiation;	GO:0005576//extracellular region;GO:0016020//membrane;GO:0016021//integral component of membrane;GO:0110165//cellular anatomical entity;	GO:0005044//scavenger receptor activity;	ko04970(Salivary secretion)
ENSMUSG00000071553	GO:0006508//proteolysis;	GO:0005576//extracellular region;GO:0005615//extracellular space;	GO:0004180//carboxypeptidase activity;GO:0004181//metallocarboxypeptidase activity;GO:0008233//peptidase activity;GO:0008237//metallopeptidase activity;GO:0008270//zinc ion binding;GO:0016787//hydrolase activity;GO:0046872//metal ion binding;	ko04974(Protein digestion and absorption);ko04972(Pancreatic secretion)
ENSMUSG00000000318	GO:0002248//connective tissue replacement involved in inflammatory response wound healing;	GO:0009897//external side of plasma membrane;GO:0016020//membrane;GO:0016021//integral component of membrane;	GO:0030246//carbohydrate binding;	–
ENSMUSG00000025163	GO:0002250//adaptive immune response;GO:0002376//immune system process;GO:0048873//homeostasis of number of cells within a tissue;	GO:0016020//membrane;GO:0016021//integral component of membrane;	GO:0038023//signaling receptor activity;	ko04640(Hematopoietic cell lineage)
ENSMUSG00000062082	GO:0150077//regulation of neuroinflammatory response;	GO:0005886//plasma membrane;GO:0009897//external side of plasma membrane;GO:0009986//cell surface;GO:0016020//membrane;GO:0016021//integral component of membrane;	GO:0005515//protein binding;GO:0038023//signaling receptor activity;	ko05167(Kaposi sarcoma-associated herpesvirus infection)
ENSMUSG00000038304	GO:0002250//adaptive immune response;GO:0002376//immune system process;GO:0002385//mucosal immune response;GO:0002729//positive regulation of natural killer cell cytokine production;GO:0002819//regulation of adaptive immune response;GO:0002857//positive regulation of natural killer cell mediated immune response to tumor cell;GO:0014065//phosphatidylinositol 3-kinase signaling;GO:0016525//negative regulation of angiogenesis;GO:0031295//T cell costimulation;GO:0032729//positive regulation of interferon-gamma production;GO:0043323//positive regulation of natural killer cell degranulation;GO:0045087//innate immune response;GO:0045954//positive regulation of natural killer cell mediated cytotoxicity;GO:0050829//defense response to Gram-negative bacterium;GO:0050860//negative regulation of T cell receptor signaling pathway;GO:1900280//negative regulation of CD4-positive, alpha-beta T cell costimulation;GO:1905675//negative regulation of adaptive immune memory response;GO:2000353//positive regulation of endothelial cell apoptotic process;	GO:0005576//extracellular region;GO:0005886//plasma membrane;GO:0016020//membrane;GO:0031225//anchored component of membrane;GO:0046658//anchored component of plasma membrane;	GO:0004888//transmembrane signaling receptor activity;GO:0005102//signaling receptor binding;GO:0005515//protein binding;GO:0019900//kinase binding;GO:0023024//MHC class I protein complex binding;GO:0032393//MHC class I receptor activity;GO:0032394//MHC class Ib receptor activity;GO:0032397//activating MHC class I receptor activity;	–

gene_id	BP	CC	MF	Pathway
ENSMUSG00000009185	GO:0002548//monocyte chemotaxis;GO:0006816// calcium ion transport;GO:0006874// cellular calcium ion homeostasis;GO:0006887// exocytosis;GO:0006935// chemotaxis;GO:0006954// inflammatory response;GO:0006955//immune response;GO:0007165//signal transduction;GO:0007186//G protein-coupled receptor signaling pathway;GO:0007267//cell-cell signaling;GO:0030593// neutrophil chemotaxis;GO:0031640// killing of cells of other organism;GO:0043547// positive regulation of GTPase activity;GO:0044828// negative regulation by host of viral genome replication;GO:0045663// positive regulation of myoblast differentiation;GO:0048245// eosinophil chemotaxis;GO:0048247// lymphocyte chemotaxis;GO:0060326// cell chemotaxis;GO:0061844// antimicrobial humoral immune response mediated by antimicrobial peptide;GO:0070098// chemokine-mediated signaling pathway;GO:0070374//positive regulation of ERK1 and ERK2 cascade;GO:0071346// cellular response to interferon-gamma;GO:0071347//cellular response to interleukin-1;GO:0071356//cellular response to tumor necrosis factor;GO:1901741//positive regulation of myoblast fusion;	GO:0005576//extracellular region;GO:0005615//extracellular space;	GO:0004672// protein kinase activity;GO:0005125// cytokine activity;GO:0008009// chemokine activity;GO:0008201// heparin binding;GO:0016004// phospholipase activator activity;GO:0048020// CCR chemokine receptor binding;	ko04062(Chemokine signaling pathway);ko04061(Viral protein interaction with cytokine and cytokine receptor);ko04060(Cytokine-cytokine receptor interaction)
ENSMUSG00000009248	GO:0000122//negative regulation of transcription by RNA polymerase II;GO:0001666//response to hypoxia;GO:0001701// in utero embryonic development;GO:0001890// placenta development;GO:0006357// regulation of transcription by RNA polymerase II;GO:0007399//nervous system development;GO:0007423// sensory organ development;GO:0010626// negative regulation of Schwann cell proliferation;GO:0030154//cell differentiation;GO:0030182// neuron differentiation;GO:0035019// somatic stem cell population maintenance;GO:0045944// positive regulation of transcription by RNA polymerase II;GO:0050767//regulation of neurogenesis;GO:0060708// spongiotrophoblast differentiation;GO:0060712// spongiotrophoblast layer development;	GO:0005634//nucleus;GO:0005737// cytoplasm;GO:0090575//RNA polymerase II transcription regulator complex;	GO:0000977// RNA polymerase II transcription regulatory region sequence-specific DNA binding;GO:0000978// RNA polymerase II cis-regulatory region sequence-specific DNA binding;GO:0000981// DNA-binding transcription factor activity, RNA polymerase II-specific;GO:0001227// DNA-binding transcription repressor activity, RNA polymerase II-specific;GO:0003677// DNA binding;GO:0003700// DNA-binding transcription factor activity;GO:0043565// sequence-specific DNA binding;GO:0046983// protein dimerization activity;GO:0070888// E-box binding;GO:1990837// sequence-specific double-stranded DNA binding;	–

gene_id	BP	CC	MF	Pathway
ENSMUSG00000033576	GO:0006869//lipid transport;GO:0008150//biological_process;GO:0042157//lipoprotein metabolic process;	GO:0005575//cellular_component;GO:0005576//extracellular region;GO:0016020//membrane;GO:0016021//integral component of membrane;	GO:0003674//molecular_function;GO:0008289//lipid binding;	–
ENSMUSG00000021214	GO:0006693//prostaglandin metabolic process;GO:0006709//progesterone catabolic process;GO:0007186//G protein-coupled receptor signaling pathway;GO:0007565//female pregnancy;GO:0007567//parturition;GO:0008202//steroid metabolic process;GO:0008284//positive regulation of cell population proliferation;GO:0010942//positive regulation of cell death;GO:0016488//farnesol catabolic process;GO:0034614//cellular response to reactive oxygen species;GO:0042448//progesterone metabolic process;GO:0042574//retinal metabolic process;GO:0044597//daunorubicin metabolic process;GO:0044598//doxorubicin metabolic process;GO:0048385//regulation of retinoic acid receptor signaling pathway;GO:0050810//regulation of steroid biosynthetic process;GO:0051897//positive regulation of protein kinase B signaling;GO:0061370//testosterone biosynthetic process;GO:0071276//cellular response to cadmium ion;GO:0071277//cellular response to calcium ion;GO:0071372//cellular response to follicle-stimulating hormone stimulus;GO:0071379//cellular response to prostaglandin stimulus;GO:0071384//cellular response to corticosteroid stimulus;GO:0071394//cellular response to testosterone stimulus;GO:0071395//cellular response to jasmonic acid stimulus;GO:0071560//cellular response to transforming growth factor beta stimulus;GO:0071799//cellular response to prostaglandin D stimulus;GO:0097211//cellular response to gonadotropin-releasing hormone;GO:1900053//negative regulation of retinoic acid biosynthetic process;GO:1904322//cellular response to forskolin;GO:1990646//cellular response to prolactin;GO:2000224//regulation of testosterone biosynthetic process;GO:2000353//positive regulation of endothelial cell apoptotic process;GO:2000379//positive regulation of reactive oxygen species metabolic process;	GO:0005634//nucleus;GO:0005737//cytoplasm;GO:0005829//cytosol;	GO:0001758//retinal dehydrogenase activity;GO:0004032//alditol:NADP+ 1-oxidoreductase activity;GO:0004033//aldo-keto reductase (NADP) activity;GO:0004745//NAD-retinol dehydrogenase activity;GO:0016229//steroid dehydrogenase activity;GO:0016491//oxidoreductase activity;GO:0016655//oxidoreductase activity, acting on NAD(P)H, quinone or similar compound as acceptor;GO:0018636//phenanthrene 9,10-monooxygenase activity;GO:0032052//bile acid binding;GO:0035410//dihydrotestosterone 17-beta-dehydrogenase activity;GO:0045550//geranylgeranyl reductase activity;GO:0045703//ketoreductase activity;GO:0047006//17-alpha,20-alpha-dihydroxypregn-4-en-3-one dehydrogenase activity;GO:0047020//15-hydroxyprostaglandin-D dehydrogenase (NADP+) activity;GO:0047023//androsterone dehydrogenase activity;GO:0047086//ketosteroid monooxygenase activity;GO:0047787//delta4-3-oxosteroid 5beta-reductase activity;	ko00140(Steroid hormone biosynthesis)
ENSMUSG00000053399	GO:0001654//eye development;GO:0006508//proteolysis;GO:0030198//extracellular matrix organization;GO:0090331//negative regulation of platelet aggregation;	GO:0005576//extracellular region;GO:0005634//nucleus;GO:0031012//extracellular matrix;	GO:0004222//metalloendopeptidase activity;GO:0008233//peptidase activity;GO:0008237//metallopeptidase activity;GO:0016787//hydrolase activity;GO:0046872//metal ion binding;	–

immunohistochemical validation. As shown in Fig. 7A, the expression levels of Lgr5 and Ascl2 were significantly lower in the DSS group than in the NC group. However, after the DSS group mice were treated with gypenosides, the expression levels of these two genes increased significantly ($P < 0.05$). This trend is consistent with the transcriptome sequencing data, indicating that gypenosides may alleviate colitis in mice by modulating the expression of Lgr5 and Ascl2.

Spearman's correlation of Lgr5, Ascl2, and differentially abundant metabolites

To determine the correlations among Lgr5, Ascl2, and differentially abundant metabolites, Spearman's correlation analysis was conducted using spearman's rank correlation coefficient. We performed Spearman correlation hierarchical clustering analysis on the two omics elements and presented the results in the form of a correlation hierarchical clustering heatmap. The results revealed that Lgr5 and Ascl2 levels were positively correlated with the relative abundance of glutamine, whereas Lgr5 and Ascl2 levels were negatively correlated with the level of arginine, which plays a role in intestinal homeostasis (Fig. 7B).

Discussion

Current medications for UC often lead to multiple side effects and complications with prolonged use. Hence, new treatments derived from natural products for the clinical management of this disease are urgently needed. In this study, we validated the intestinal protective effect of gypenosides and explored the underlying mechnisms via transcriptomics and metabolomics, providing experimental evidence for its potential as a novel therapeutic agent against UC. We used a DSS-induced mice model to simulate the typical clinical conditions of UC, and elucidated the drug-transcriptomic/ metabolomic-disease interactions. Our findings confirm the intestinal protective effects of gypenosides. Treatment with a 400 mg/kg gypenosides solution alleviated colitis symptoms in UC model mice, as evidenced by increased body weight and colon length, and reduced histological tissue inflammation. Moreover, drug intervention effectively reduced the expression levels of inflammatory cytokines (IL-6 and TNF-α) in UC model mice. As a natural product, gypenosides are both cost-effective and relatively safe, making them a promising alternative or supplementary therapy for UC treatment. To elucidate the therapeutic mechanisms of gypenosides in UC, we conducted comprehensive metabolomic and transcriptomic analyses. Transcriptomic analysis revealed that the intestinal stem cell markers Ascl2 and Lgr5 were restored to normal levels by gypenosides treatment. The expression of Ascl2 and Lgr5 in the DSS mice was significantly lower than that in the NC group. However, the administration of gypenosides abrogated this downwards trend in expression. In summary, our findings offer substantial evidence demonstrating the beneficial effects of gypenosides in alleviating UC and clarify the underlying mechanisms that support its clinical application.

Previously, Ascl2 and Lgr5 were shown to be critical markers for intestinal stem cells (ISCs) and to play important roles in maintaining intestinal homeostasis and regeneration[17]. Lgr5 is expressed primarily on the cell surface of the intestine, and has been identified as a specific marker for crypt-base columnar cells (CBCs) in mice[20]. Lgr5 + intestinal stem cells (ISCs) are intricately regulated by the Wnt/β-catenin and Notch signalling pathways to maintain their self-renewal and differentiation functions, thereby sustaining crypt homeostasis and repairing intestinal mucosal damage[21]. This process is crucial for the homeostatic regeneration of the small intestine and colon. Moreover, Ascl2 is a transcription factor crucial for the maintenance and proliferation of intestinal stem cells, which that drives expression of Lgr5 gene[22]. The interaction between Ascl2 and Lgr5 is crucial for sustaining a population of active intestinal stem cells, which are vital for the ongoing renewal of the intestinal lining[23–25]. The increased interest in intestinal dryness has opened new avenues for the clinical treatment of UC. We performed immunohistochemistry validation and demonstrated that the ameliorative effect of gypenosides on colitis in mice might occur through the regulation of Lgr5 and Ascl2 expression, thereby affecting intestinal stem cell function.

Previous studies have shown that Ascl2 and Lgr5 together regulate the metabolic pathways of intestinal stem cells, including glycolysis, lipid metabolism, and amino acid metabolism[26]. These pathways provide the energy and building blocks necessary to support the efficient proliferation and differentiation of stem cells. In this study, the metabolomic analysis revealed significant pattern differences between UC model mice and those treated with gypenosides, indicating that metabolic disturbances during UC progression were abrogated by gypenosides intervention. Compared with UC model mice, mice treated with gypenosides presented significant differences in metabolic pathways related to amino acid metabolism. Previous studies have indicated that amino acid metabolism is associated with the development of colitis in UC patients, primarily involving pathways such as 'aminoacyl-tRNA biosynthesis', 'arginine biosynthesis', 'alanine, aspartate, and glutamate metabolism', 'biosynthesis of unsaturated fatty acids', 'valine, leucine, and isoleucine biosynthesis', and 'pantothenate and CoA biosynthesis'. Glutamine is a vital fuel source for enterocytes (intestinal epithelial cells) and plays a crucial role in maintaining the integrity and function of the intestinal barrier[27]. It supports the proliferation and differentiation of enterocytes, thereby reinforcing the mucosal lining of the gut. The combined analysis results further revealed a positive correlation between intestinal stem cell markers and glutamine levels. The rapid proliferation of intestinal stem cells requires a large supply of glutamine, which serves not only as a crucial amino acid for protein synthesis but also for energy metabolism and cell signalling. Glutamine acts as a nutrient sensor, influencing intestinal stem cell proliferation and differentiation by regulating pathways such as mTOR signalling[28–30]. Additionally, glutamine exerts strong antioxidant properties effects in the intestine, helping to reduce oxidative stress damage to intestinal stem cells and protecting them from environmental stimuli[31–34]. Although positively correlated with glutamine, Lgr5 and Ascl2 are negatively correlated with arginine. Arginine metabolism may lead to changes in the cellular metabolic state, affecting the transcriptional activity of Ascl2 [21]. For example, metabolites of arginine may inhibit Ascl2 expression by regulating the intracellular environment and signalling pathways[35,36]. Arginine plays a crucial role in immune cell function and inflammatory responses, which may indirectly regulate Lgr5 expression by affecting the homeostasis of the intestinal microenvironment[37]. Moreover,

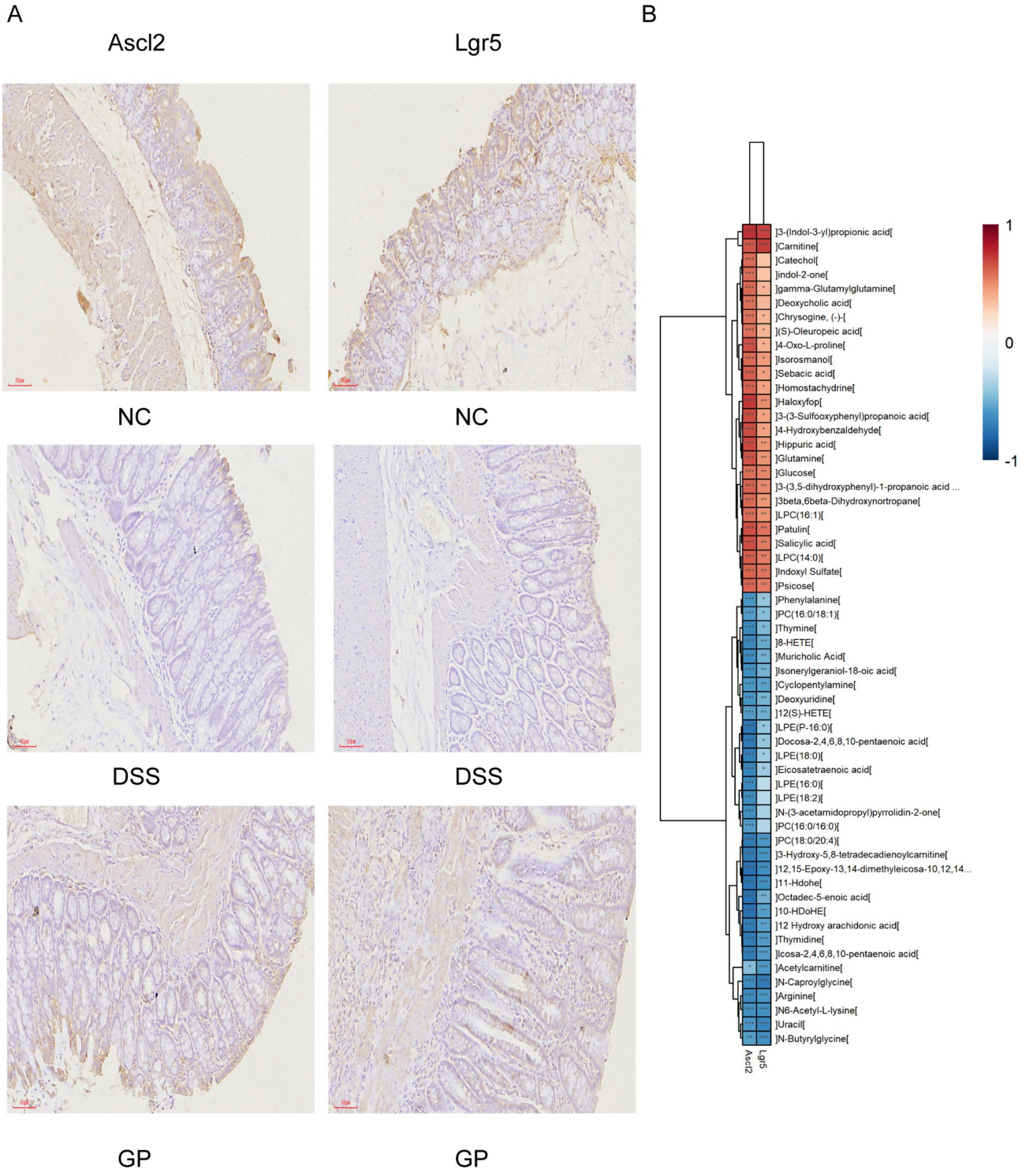

Fig. 7. Experimental verification of key genes and analysis of their correlation with metabolism. Representative image of immunohistochemical staining. (B) Spearman correlation analysis of key genes and metabolites. * $P < 0.05$, ** $P < 0.01$, *** $P < 0.001$.

changes in the inflammatory response and immune status can influence the expression of genes, including Lgr5, in intestinal stem cells[38]. The relevant mechanisms are worth further exploration.

We have preliminarily confirmed the mechanism by which gypenosides in treat UC. However, our study also has certain limitations. First, integrated analyses of transcriptomics and metabolomics often rely on existing databases. These databases may not fully cover all genes and metabolites. Second, individual biological differences can affect the reliability of transcriptomic and metabolomic data. Large sample sizes are needed to control and correct for this variability. Besides, gypenosides may confer intestinal protection through the modulation of

intestinal stem cells, the potential secondary regulatory effects on gut function mediated by their central anti-inflammatory actions via the brain-gut axis remain poorly characterized.Finally, gypenosides reduces colonic inflammation and improves UC symptoms. However, direct evidence for remission induction and the efficacy and safety require further validation in acute-phase models or clinical trials with earlier intervention.

Conclusion

In conclusion, we observed that gypenosides treatment alleviated DSS-induced colitis, with this effect correlating with altered expression of intestinal stem cell markers and amino acid metabolism profiles in a DSS-induced colitis mouse model.

Data availability

Data is provided within the manuscript or supplementary information files only for review. The sequencing datasets generated and analyzed during the current study are not publicly available as the research team is still conducting further data analysis and exploring underlying mechanisms. However, the data are available from the corresponding author upon reasonable request.

Received: 4 August 2024; Accepted: 7 July 2025
Published online: 29 August 2025

References

1. Mak, W. Y., Zhao, M., Ng, S. C. & Burisch, J. The epidemiology of inflammatory bowel disease: East Meets West. *J. Gastroenterol. Hepatol.* **35**, 380–389 (2020).
2. Xavier, R. J. & Podolsky, D. K. Unravelling the pathogenesis of inflammatory bowel disease. *Nature* **448**, 427–434 (2007).
3. Torres, J., Mehandru, S. & Colombel, J. F. Peyrin-Biroulet, L. Crohn's disease. *Lancet* **389**, 1741–1755 (2017).
4. Su, C. et al. Progress in the medicinal value, bioactive compounds, and Pharmacological activities of gynostemma pentaphyllum. *Molecules* **26**, 6249 (2021).
5. Huang, W. C. et al. Extract of gynostemma pentaphyllum enhanced the production of antibodies and cytokines in mice. *Yakugaku Zasshi-J Pharm. Soc. Jpn.* **127**, 889–896 (2007).
6. Xia, X. et al. Gypenosides pretreatment alleviates the cerebral ischemia injury via inhibiting the Microglia-Mediated neuroinflammation. *Mol. Neurobiol.* **61**, 1140–1156 (2024).
7. Zhang, X. et al. Anti-inflammatory, cardioprotective effect of gypenosides against isoproterenol-induced cardiac remodeling in rats via alteration of inflammation and gut microbiota. *Inflammopharmacology* **31**, 2731–2750 (2023).
8. Zhang, H. K., Ye, Y., Li, K. J., Zhao, Z. N. & He, J. F. Gypenosides prevent H_2O_2-Induced retinal ganglion cell apoptosis by concurrently suppressing the neuronal oxidative stress and inflammatory response. *J. Mol. Neurosci.* **70**, 618–630 (2020).
9. Wu, H. et al. Gypenosides induces apoptosis by inhibiting the PI3K/AKT/mTOR pathway and enhances T-cell antitumor immunity by inhibiting PD-L1 in gastric cancer. *Front. Pharmacol.* **15**, 1243353 (2024).
10. Zhang, H. et al. Gypenosides improve diabetic cardiomyopathy by inhibiting ROS-mediated NLRP3 inflammasome activation. *J. Cell. Mol. Med.* **22**, 4437–4448 (2018).
11. Li, H., Xi, Y., Xin, X., Tian, H. & Hu, Y. Gypenosides regulate farnesoid X receptor-mediated bile acid and lipid metabolism in a mouse model of non-alcoholic steatohepatitis. *Nutr. Metab. (Lond).* **17**, 34 (2020).
12. Shen, S., Wang, K., Zhi, Y. & Dong, Y. Gypenosides counteract hepatic steatosis and intestinal barrier injury in rats with metabolic associated fatty liver disease by modulating the adenosine monophosphate activated protein kinase and Toll-like receptor 4/nuclear factor kappa B pathways. *Pharm. Biol.* **60**, 1949–1959 (2022).
13. Huang, X. et al. Gypenosides improve the intestinal microbiota of non-alcoholic fatty liver in mice and alleviate its progression. *Biomed. Pharmacother.* **118**, 109258 (2019).
14. Zhu, X. et al. Multi-omics approaches for in-depth Understanding of therapeutic mechanism for traditional Chinese medicine. *Front. Pharmacol.* **13**, 1031051 (2022).
15. Jiashuo, W. U., Fangqing, Z., Zhuangzhuang, L. I., Weiyi, J. & Yue, S. Integration strategy of network Pharmacology in traditional Chinese medicine: a narrative review. *J. Tradit. Chin. Med.* **42**, 479–486 (2022).
16. Zhu, Y. et al. New opportunities and challenges of natural products research: when target identification Meets single-cell multiomics. *Acta Pharm. Sin. B.* **12**, 4011–4039 (2022).
17. Leung, C., Tan, S. H. & Barker, N. Recent advances in $Lgr5^+$ stem cell research. *Trends Cell. Biol.* **28**, 380–391 (2018).
18. Zhang, J. et al. Vitexin protects against dextran sodium Sulfate-Induced colitis in mice and its potential mechanisms. *J. Agric. Food Chem.* **70**, 12041–12054 (2022).
19. Erben, U. et al. A guide to histomorphological evaluation of intestinal inflammation in mouse models. *Int. J. Clin. Exp. Pathol.* **7**, 4557–4576 (2014).
20. Barker, N. et al. Identification of stem cells in small intestine and colon by marker gene Lgr5. *Nature* **449**, 1003–1007 (2007).
21. Schuijers, J. et al. Ascl2 acts as an R-spondin/Wnt-responsive switch to control stemness in intestinal crypts. *Cell. Stem Cell.* **16**, 158–170 (2015).
22. Strubberg, A. M. et al. The zinc finger transcription factor PLAGL2 enhances stem cell fate and activates expression of Ascl2 in intestinal epithelial cells. *Stem Cell. Rep.* **11**, 410–424 (2018).
23. Zheng, L., Duan, S. L., Wen, X. L. & Dai, Y. C. Molecular regulation after mucosal injury and regeneration in ulcerative colitis. *Front. Mol. Neurosci.* **9**, 996057 (2022).
24. Murata, K. et al. Ascl2-Dependent cell dedifferentiation drives regeneration of ablated intestinal stem cells. *Cell. Stem Cell.* **26**, 377–390 (2020).
25. Wu, L. et al. Ascl2 affects the efficacy of immunotherapy in Colon adenocarcinoma based on Single-Cell RNA sequencing analysis. *Front. Immunol.* **13**, 829640 (2022).
26. Yan, K. S. et al. Intestinal enteroendocrine lineage cells possess homeostatic and Injury-Inducible stem cell activity. *Cell. Stem Cell.* **21**, 78–90 (2017).
27. Liu, M., Guo, S. & Wang, L. Systematic review of metabolomic alterations in ulcerative colitis: unveiling key metabolic signatures and pathways. *Th. Adv. Gastroenterol.* **17**, 17562848241239580 (2024).
28. Moore, S. R. et al. Glutamine and alanyl-glutamine promote crypt expansion and mTOR signaling in murine enteroids. *Am. J. Physiol. Gastrointest. Liver Physiol.* **308**, G831–839 (2015).
29. Boukhettala, N. et al. Effects of essential amino acids or glutamine deprivation on intestinal permeability and protein synthesis in HCT-8 cells: involvement of GCN2 and mTOR pathways. *Amino Acids.* **42**, 375–383 (2012).
30. Tian, Y., Wang, K., Wang, Z., Li, N. & Ji, G. Chemopreventive effect of dietary glutamine on colitis-associated colon tumorigenesis in mice. *Carcinogenesis* **34**, 1593–1600 (2013).

31. Xu, C. L. et al. Protective effect of glutamine on intestinal injury and bacterial community in rats exposed to hypobaric hypoxia environment. *World J. Gastroenterol.* **20**, 4662–4674 (2014).
32. Soares, A. D. et al. Dietary glutamine prevents the loss of intestinal barrier function and attenuates the increase in core body temperature induced by acute heat exposure. *Br. J. Nutr.* **112**, 1601–1610 (2014).
33. Gu, A., Yang, L., Wang, J., Li, J. & Shan, A. Protective effect of glutamine and alanyl-glutamine against zearalenone-induced intestinal epithelial barrier dysfunction in IPEC-J2 cells. *Res. Vet. Sci.* **137**, 48–55 (2021).
34. Wang, B. et al. Glutamine and intestinal barrier function. *Amino Acids*. **47**, 2143–2154 (2015).
35. Baier, J. et al. Arginase impedes the resolution of colitis by altering the Microbiome and metabolome. *J. Clin. Invest.* **130**, 5703–5720 (2020).
36. Hou, Q. et al. Regulation of the Paneth cell niche by exogenous L-arginine couples the intestinal stem cell function. *FASEB J.* **34**, 10299–10315 (2020).
37. Hou, Q. et al. Exogenous L-arginine increases intestinal stem cell function through CD90 + stromal cells producing mTORC1-induced Wnt2b. *Commun. Biol.* **3**, 611 (2020).
38. Martí, I. L. A. A. & Reith, W. Arginine-dependent immune responses. *Cell. Mol. Life Sci.* **78**, 5303–5324 (2021).

Author contributions

(I) Conception and design: Yuan Yang, Xinyuan Li, Fan Huang. (II) Administrative support: Guangsheng Hu, Bin Zeng, Weiwei Zhou, Yuan Yang. (III) Provision of study materials: Fuchao Cai, Qilin Jiang. (IV) Collection and assembly of data: Xinyuan Li, Fan Huang, Fuchao Cai, Xufeng Ning. (V) Data analysis and interpretation: Lingshan Zhou, Yuan Yang. (VI) Manuscript writing: All authors. (VII) Final approval of manuscript: All author.

Funding

This study was supported by Scientific Research Fund Project of Hunan Provincial Health Commission (20233462), The Research Foundation of Education Bureau of Hunan Province (23A0347), and Natural Science Foundation of Gansu province (22JR5RA889, 22JR11RA031).

Declarations

Competing interests

The authors declare no competing interests.

Additional information

Supplementary Information The online version contains supplementary material available at https://doi.org/10.1038/s41598-025-11010-0.

Correspondence and requests for materials should be addressed to B.Z., W.Z. or G.H.